Manila Journal of Science 9 (2016), pp. 148-155

Density Functional Theory–Based Study of the Structural Properties of *Hexagonal* Boron Nitride/Graphene Hetero-Bilayer and Silicene/*Hexagonal* Boron Nitride/Graphene Hetero-Structures for Thin Film Transistor Applications

Carlo Angelo Pelotenia[1*], Allan Abraham Padama[2], Susan Aspera[7],
Nelson Arboleda, Jr.[1, 3, 4], Hideaki Kasai[5, 6, 7], Melanie David[1, 4]

[1]Physics Department, De La Salle University, Taft Avenue, 0922 Manila, Philippines
[2]Physics Department, University of the Philippines, Los Baños, Laguna, Philippines
[3]De La Salle University- Science and Technology Complex, Biñan, Laguna, Philippines
[4]Center for Natural Sciences & Environmental Research, Computational Materials Design Unit, De La Salle University, Philippines
[5]Division of Precision Science and Technology and Applied Physics, Graduate School of Engineering, Osaka University, 2-1 Yamadaoka, Suita, Osaka 5650871, Japan
[6]Institute of Industrial science, The University of Tokyo, Meguro-Ku, Tokyo 153-8505, Japan
[7]National Institute of Technology, Akashi, Japan

*Corresponding author: carlo_angelo_pelotenia_a@dlsu.edu.ph

ABSTRACT

The geometric properties and structural stability of hexagonal boron nitride on graphene (*h*-BN/G) hetero-bilayer and silicene on hexagonal boron nitride on graphene (Si/*h*-BN/G) hetero-structure were investigated using density functional theory. The calculations were performed through the Vienna Ab Initio Simulation package (VASP) implemented with three different approximations, namely, the local density approximation (LDA), general gradient approximation (GGA), and GGA with Tkatchenko–Scheffler van der Waals (vdW) correction. In reference to the experimental interlayer distance and binding energy between graphitic layers, the *h*-BN/G hetero-bilayer and Si/*h*-BN/G hetero-structures were stable. Moreover, it was found that among all functional approximations tested, the one with the vdW correction was the most precise relative to experiments.

Keywords: silicene; graphene; boron nitride; hetero-structure; transistor

INTRODUCTION

Graphene is a two-dimensional nanomaterial formed by carbon atoms with sp^2-hybridization that has a very stable lattice structure, high thermal conductivity, and high carrier mobility and with massless Dirac fermions (Geim, 2009). It is believed to form smaller yet stable transistors with impressive electronics that can improve computational power (Ladd et al., 2010). However, its lack of band gap and low affinity with the existing semiconducting circuits drove scientists to conduct further research for other noble materials (Geim, 2009; Ladd et al., 2010).

One of the two-dimensional atomic planes that are similar to graphene is silicene. Its hexagonal lattice is composed of silicon atoms with sp^3-hybridization. Theoretically, it has the same significant characteristics as mentioned above (Sahin & Peeters, 2013; Vogt et al., 2012). In addition, it is compatible with existing electronic devices, with a high on/off ratio, electrically tunable band gap, and electrically induced ability to shift from a topological insulator to a band insulator (Aufray et al., 2010). These characteristics made silicene a potential substitute for graphene.

However, silicene is not as stable as graphene and cannot exist in a free-standing state (Vogt et al., 2012; Aufray et al., 2010; Guo et al., 2013; Morishita et al., 2013; Fleurence et al., 2013). It was computationally and experimentally studied to form on metallic substrates such as Ag (110) (Vogt et al., 2012; Aufray et al., 2010), Ag (111) (Guo et al., 2013), Al (111) (Morishita et al., 2013), and ZrB_2 (Fleurence et al., 2012) However, these metallic substrates interact strongly with silicene and create undesirable symmetry breaking resulting to the disappearance of some of its valuable properties such as Dirac fermions. These studies implied that silicene cannot be separated from its substrate due to strong interaction.

Different processes such as incorporating dopants, adatoms, and vacancies were performed on these nanomaterials to provide functionalization (Aufray et al., 2010; Bandura & Pichanusakorn, 2010). However, these processes provided limited insights to the functionalization of these materials in relation to direct application to electronic devices. Recently, another process that involved the stacking of atomic planes on top of each other, layer by layer like LEGOS™, was introduced (Geim & Grigorieva, 2013). These heterostructures are very similar to graphite wherein in-plane stability is provided by strong covalent bonds while relatively weak van der Waals forces are enough to hold these layers on top of one another (Geim & Grigorieva, 2013). These weak interlayer interactions are due to the dangling $2p_z$-orbitals of graphene layers of graphite (Reynolds, 1968), which are also present in other atomic planes like silicene (Cahangirov et al., 2009). In addition, this layer-by-layer stacking is similar to the arrangement of thin film transistors (TFTs) synthesized in an epitaxial manner. As shown in Figure 1, TFT has three major parts: the conducting gate, the insulating dielectric, and

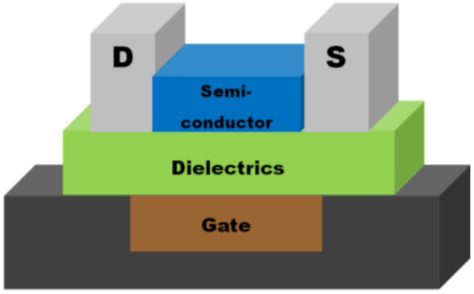

Figure 1. Schematic image of a staggered bottom-gate thin-film transistor.

the semiconducting part. With this layer-by-layer stacking, the interaction mechanism of atomic planes can be investigated for the miniaturization of the parts of a TFT.

Graphene, having a high transparency, high carrier mobility, high flexibility, high stability, and high conductivity, has a great potential for the conducting gate material of a thin film transistor (Yan et al., 2012). On the other hand, silicene is also flexible and transparent and has high carrier mobility (Sahin & Peeters, 2013; Fleurence et al., 2012). Moreover, silicene has a tunable band gap and high on/off ratio, which are properties needed for the TFT's semiconducting part. However, since silicene interacts strongly with metallic materials (Vogt et al., 2012; Aufray et al., 2010; Guo et al., 2013; Morishita et al., 2013; Fleurence et al., 2013) such as graphene, a buffer layer in between them is required. In a previous study, silicene was found to interact weakly with hexagonal boron nitride (*h*-BN). It was said that its intrinsic electronic properties are preserved (Kaloni et al., 2013). This is also true for the interaction of graphene with *h*-BN (Giovanetti et al., 2007). The honeycomb lattice structure of *h*-BN, which matches that of graphene and silicene, made it a more fitted intercalating material for the system. Furthermore, it was found that *h*-BN was an ultrathin and high-quality two-dimensional material with a low dielectric constant barrier. This implies that it has a great potential in application to noble electron tunneling devices and for investigating strongly coupled and narrowly separated electrodes of different composition (Britnell et al., 2012). These findings support the suitability of *h*-BN as the buffer layer and dielectric material between silicene and graphene in the hetero-structure for TFT application.

By employing density-functional-based calculations, the geometric structure and stability of hexagonal boron nitride on graphene (*h*-BN/G) hetero-bilayer and silicene on hexagonal boron nitride on graphene (Si/*h*-BN/G) hetero-structure were investigated for thin film transistor application. In addition, the calculations were performed using local density approximation (LDA; Kohn & Sham, 1965), generalized gradient approximation given by Perdew–Burke–Ernzerhof (PBE; Perdew, Burke, & Ernzerhof, 1996), and PBE with Tkatchenko–Scheffler van der Waals correction with self-consistent screening (PBE TS+SCS; Tkatchenko et al., 2012) to provide comparative information.

MATERIALS AND METHODS

A (1x1) *hexagonal* boron nitride (*h*-BN) was placed on (1x1) honeycomb graphene to form the hetero-bilayer. On the other hand, silicene was positioned on top of the *h*-BN/G hetero-bilayer for the Si/*h*-BN/G hetero-structure. This super cell is composed of (2x2) honeycomb silicene on (3x3) *h*-BN (with 9 boron and 9 nitrogen atoms) on (3x3) honeycomb graphene.

All calculations implemented in this study were based on density functional theory (DFT) using the Vienna Ab-initio simulation package (VASP; Kresse & Furthmuller, 1996) employed in three exchange correlation functionals: local density approximation (LDA; Kohn & Sham, 1965), generalized gradient approximation given by PBE (Perdew, Burke, & Ernzerhof, 1996), and PBE TS+SCS (Tkatchenko et al., 2012). The projected augmented wave (PAW) method (Kresse & Joubert, 1999) was used to describe ionic cores. On the other hand, an energy cutoff of at least 800eV and a 16x16x1 k-point mesh were utilized to acquire an energy and force precision of 10-5eV and -0.03eV/Å, respectively. For the super cell, a minimum of 17Å vacuum layer along the direction perpendicular to the atomic planes was implemented in order to minimize the interaction between the adjacent unit cells along the said direction. The geometric structures were viewed through Visualization for Electronic and Structural Analysis (VESTA; Momma & Izumi, 2008).

RESULTS AND DISCUSSION

A. Hexagonal Boron Nitride/Graphene (*h*-BN/G) Hetero-Bilayer

In this structure, the super cell has (1x1) *hexagonal* boron nitride (*h*-BN) placed on (1x1) honeycomb graphene at different stacking arrangements as shown in Figure 2. The first stacking, noted as Boron and Nitrogen atoms on Graphene or BNG, shows that all the boron and nitrogen atoms are on top of carbon atoms. In the second stacking, Boron atoms on Graphene or BG, the boron atoms are on top of carbon atoms while nitrogen atoms are on top of the center of graphene hexagonal rings. Lastly, the third stacking, which is the Nitrogen on Graphene or NG, shows that the nitrogen atoms are on top of the carbon atoms while boron atoms are on top of the center of graphene rings.

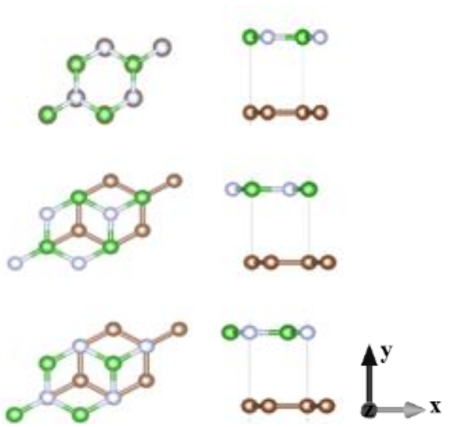

Figure 2. *h*-BN/G hetero-bilayer stacking.

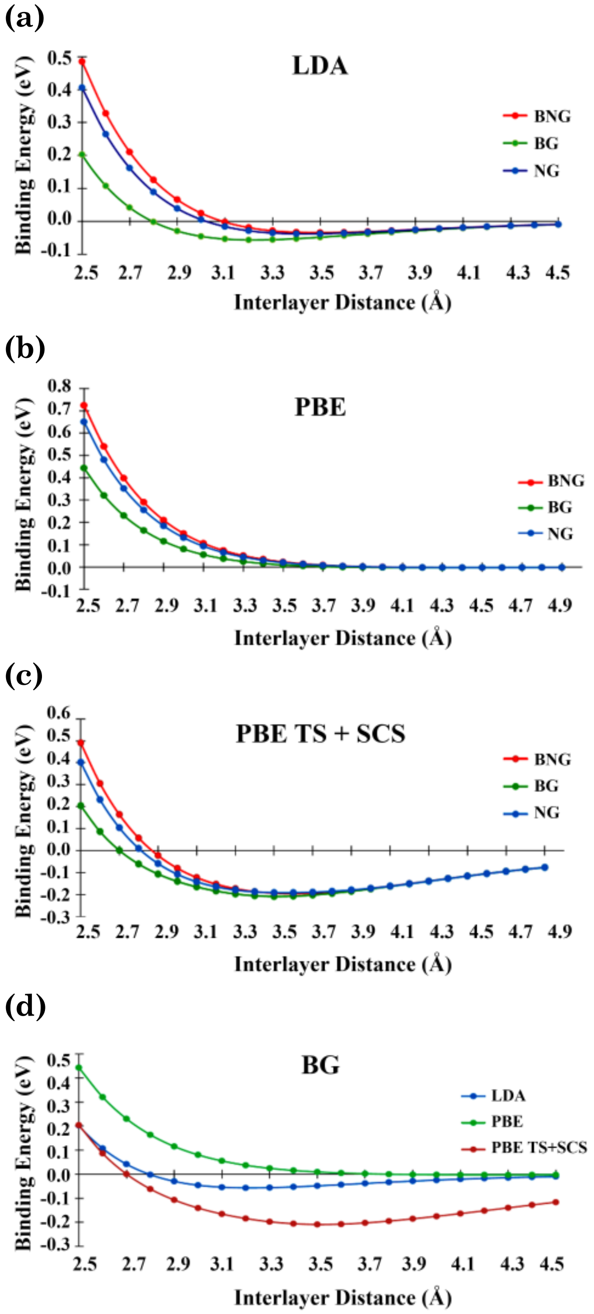

Figure 3. Binding energy versus interlayer distance of *h*-BN/G hetero-bilayer with different stacking arrangement.

To identify the preferred stacking arrangement of the *h*-BN/G hetero-bilayer, the total binding energy for each arrangement was calculated and plotted as a function of the interlayer distance between the *h*-BN sheet and graphene sheet. As shown in Figure 3 (a–c), these energies were calculated with (a) LDA, (b) PBE, and (c) PBE TS+SCS functional approximations for BNG Stacking (red), NG stacking (blue), and BG stacking (green). It can be seen that for different exchange-correlation functionals, BG stacking has the lowest energy configuration. This implies that the *h*-BN/G hetero-bilayer always prefers the BG stacking.

From Table 1, LDA and PBE TS+SCS give precise values for the interlayer distance between *h*-BN and graphene relative to the existing experimental data. However, LDA underestimates the binding energy between the atomic planes while PBE TS+SCS gives a more precise result especially for the binding energy of the atomic planes in BG stacking arrangement. This is evident in Figure 3 (d). The PBE functional underestimation of the binding energy resulted into an overestimation of the interlayer distance between the atomic planes. The precision of the calculation with van der Waals correction suggests that the van der Waals force is significant in the interaction between *h*-BN and graphene. Consequently, since the calculated interlayer distance and binding energy is very precise with the experimental data, it can be inferred that the *h*-BN/G hetero-bilayer is structurally stable.

Adapted from a previous study (Lalmi et al., 2010), the lattice mismatch (Δ) between these atomic planes is defined as $\Delta = \frac{|a_{BN}-a_G|}{a_G} \times 100\%$ where a_G is the lattice constant of graphene while a_{BN} is the lattice constant of *h*-BN. The values of the lattice mismatch between *h*-BN and graphene using LDA, PBE, and PBE TS+SCS are 1.65%, 1.79%, and 1.75%, respectively. These resulted to the shortening of the bond length of *h*-BN by 1.79%. However, the rest of the geometric parameters of *h*-BN and graphene remain unchanged. Thus, relative to their computed free-standing states, there is no major distortion in the geometric structures of *h*-BN and graphene due to lattice mismatch, suggesting that these atomic planes fit well. Consequently, this indicates that the van der Waals force bonded the *h*-BN and graphene without significantly changing their geometric properties.

Table 1. The Computed Interlayer Distance and Binding Energies of h-BN/G Hetero-Bilayer in Different Stacking Arrangements Under the LDA, PBE, and PBE TS+SCS Approximations

	Interlayer Distance (Å)			
	LDA	**PBE**	**PBE+TS SCS**	**Expt.**
BNG	3.50	4.49	3.59	3.34[a]
BG	3.22	4.30	3.52	
NG	3.44	4.48	3.56	

[a]Experimental (Expt.) result for graphite's interlayer distance by Baskin & Meyer, 1955.

	Interlayer Binding Energy (meV/atom)			
	LDA	**PBE**	**PBE+TS SCS**	**Expt.**
BNG	8.64	0.60	46.87	52±5[b]
BG	14.21	0.73	50.13	
NG	9.53	0.60	45.92	
NG	3.44	4.48	3.56	

[b] Experimental result for graphite's interlayer binding energy by Zacharia et al., 2004.

B. Silicene/Hexagonal Boron Nitride/ Graphene (Si/*h*-BN/G) Hetero-Structure

Figure 4 (a–b) shows silicene placed on top of the *h*-BN/G hetero-bilayer in BG stacking arrangement. The super cell is composed of (2x2) honeycomb silicene on (3x3) *h*-BN (with 9 boron and 9 nitrogen atoms) on (3x3) honeycomb graphene. The lattice mismatch

(Δ) between the atomic planes is defined as $\frac{|(3\times a_{BN/G})-(2\times a_{Si})|}{(2\times a_{Si})}\times 100\%$, where $a_{BN/G}$ is the lattice constant of the *h*-BN/G hetero-bilayer while a_{Si} is the lattice constant of silicene (Lalmi et al., 2010). The values of the lattice mismatch between *h*-BN/G hetero-bilayer and silicene using LDA, PBE, and PBE TS+SCS is 4.00%, 4.09%, and 4.31%, respectively. In PBE TS+SCS, graphene's bond length and buckling remain unchanged. However, due to large lattice mismatch, the bond length of *h*-BN and silicene shortened by 1.78% and 2.546%, respectively. In terms of buckling, *h*-BN and graphene were unchanged. On the other hand, the buckling of silicene increased by 0.16Å. These can be attributed to the fact that the lattice constant of silicene is almost twice that of *h*-BN and graphene.

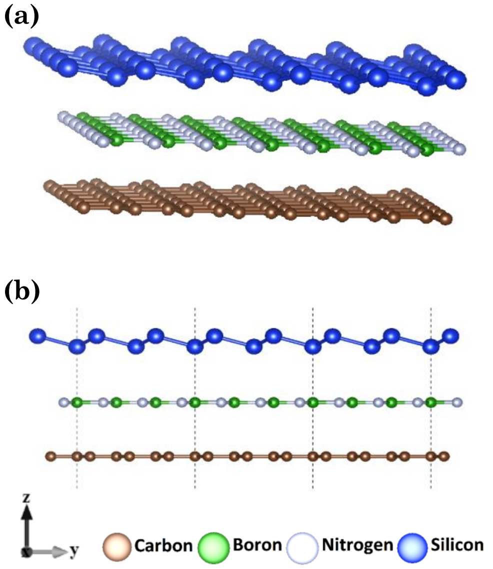

Figure 4. Optimized (a) geometric structure and (b) unit cell of Si/h-BN/G hetero-structure.

In Table 2, PBE overestimated the interlayer distance of silicene from the *h*-BN/G hetero-bilayer. Consequently, it underestimated the interlayer binding energy. On the other hand, the calculated interlayer distances with LDA (3.43Å) and PBE TS+SCS (3.50Å) approximations are close to one another. However, PBE TS+SCS approximated the binding energy almost thrice the approximated value of LDA. Among the three functionals, the binding energy calculated with PBE TS+SCS is the most precise relative to the binding energy of graphite, which is 52±5meV/atom (Zacharia et al., 2004). This infers that the Si/*h*-BN/G hetero-structure can stably form with atomic planes interacting via van der Waals force.

	Interlayer Distance (Å)			
	LDA	**PBE**	**PBE+TS SCS**	**Expt.**
Si/*h*-BN/G	3.43	4.31	3.50	3.34[a]

	Interlayer Binding Energy (meV/atom)			
	LDA	**PBE**	**PBE+TS SCS**	**Expt.**
Si/*h*-BN/G	9.20	0.42	61.09	52±5[b]

CONCLUSION

The geometric properties of *h*-BN/G hetero-bilayer and the geometric properties of Si/*h*-BN/G hetero-structure were investigated using density functional theory. It was found that vdW force has a significant role in the interaction of layered hetero-structures. Thus, computations of layered systems must be done with vdW corrections. Results showed that *h*-BN/G hetero-structure and Si/*h*-BN/G hetero-structure can geometrically form with binding energies of 50.13 and 61.09 meV/atom, respectively. Further investigations on the electronic properties of these materials must be performed to evaluate their potential applications for electronic devices.

ACKNOWLEDGMENTS

C.A. Pelotenia would like to acknowledge the Japan Student Services and Organization (JASSO) through the Quantum Engineering Design Course Short-Term Program with the Kasai–Diño Laboratory of Osaka University. Also, this study will not be possible without the support of the Physics Department at De La Salle University through the Computational Materials Design Research Group and the Center for Natural Sciences and Environmental Research through the High Performance Computing Laboratory. C.A. Pelotenia would also like to thank the Department of Science and Technology (DOST) through the Accelerated Science and Technology Human Resource Development (ASTHRD) Scholarship Program for their financial assistance. A.A.B. Padama acknowledges and is grateful to the University of the Philippines for the research support through its Foreign-Trained "Balik" PhD Program.

REFERENCES

Aufray, B., Kara, A., Vizzini, S., Oughaddou, H., & Leandri, C. (2010). Graphene-like silicon nanoribbons on Ag(110): A possible formation of silicene. *Applied Physics Letters, 96*(18)*,* 1–3.

Bandura, P., & Pichanusakorn, P. (2010, January 22). An outline of the synthesis and properties of silicon nanowires. *Semiconductor Science and Technology, 25(*2)*,* 1–16.

Baskin, Y., & Meyer, L. (1955). Lattice constants of graphite at low temperatures. *Physical Reviews*, *100*, 544.

Britnell, L., Gorbachev, R., Jalil, R., Belle, B., Schedin, F., Katnelson, M., et al. (2012). Electron tunneling through ultrathin boron nitride crystalline barriers. *Nano Letters, 12*, 1707–1710.

Cahangirov, S., Topsakal, M., Aktürk, E., Şahin, H., & Ciraci, S. (2009). Two- and one-dimensional honeycomb structures of silicon and germanium. *Physical Review Letter, 102*(23), 1–4.

Fleurence, A., Friedlien, R., Ozaki, T., Kawai, H., Wang, Y., & Yamada-Takamura, Y. (2012). Experimental evidence for epitaxial silicene on diboride thin films. *Physical Review Letters, 108*(24)*,* 1–5.

Geim, A. (2009). Graphene: Status and prospects. *Science, 324*, 1530–1534.

Geim, A. K., & Grigorieva, I. V. (2013). Van der Waals heterostructure. *Nature, 499* , 419–425.

Giovannetti, G., Khomyakov, P., Brocks, G., Kelly, P., & van der Brink, J. (2007). Substrate-induced bad gap in graphene on hexagonal boron nitride: Ab inition density functional calculations. *Physical Review B, 76*(07)*,* 1–4.

Guo, Z.-X., Furuya, S., Iwata, J.-iI., & Oshiyama, A. (2013). Absence of dirac electrons in silicene on Ag (111) surfaces. *Journal of the Physical Society of Japan, 82*(6), 1–5.

Kaloni, T., Tahir, M., & Schwingenschlogl, U. (2013). Quasi free-standing silicene in a superlattice with hexagonal boron nitride. *Scientific Reports, 3*(31)*,* 1–4.

Kohn, W., Sham, J. (1965). Self-consistent equations including exchange and correlation effects. *Physical Review, 140,* 1133–1138.

Kresse, G., & Joubert, D. (1999). From ultrasoft pseudopotentials to the projector augmented-wave method. *Physics Review B, 59,* 1758–1775.

Kresse, G., Furthmuller, J. (1996). Efficient iterative schemes for ab initio total-energy calculations using a plane-wave basis set. *Physical Review B.*, *54*(16)*,* 11169–11186.

Ladd, T., Jelezko, F., Laflamme, R., Nakamura, Y., Monroe, C., & O'Brien, J. (2010). Quantum computers. *Nature* , *465,* 45–53.

Lalmi, B., Oughaddou, H., Enriquez, H., Kara, A., Vizzini, S., Ealet, B., et al. (2010). Epitaxial growth of silicene sheet. *Applied Physics Letters, 97*(22), 1–2.

Momma, K., & Izumi, F. (2008). VESTA: a A three-dimentional visualization system for electronic and structural analysis. *Journal of Applied Crystallography, 41*, 653–658.

Morishita, T., Spencer, M., Kawamoto, S., & Snook, I. (2013). A new surface and structure for silicene: Polygonal silicene formation on the Al (111) surface. *The Journal of Physical Chemistry, 117*(42)*,* 22142–22148.

Perdew, J., Burke, K., Ernzerhof, M. (1996).

Generalized gradient approximation made simple. *Physical review Letters, 77*(18), 3865–3868.

Reynolds, W. (1968). *Physical properties of graphite.* New York: Elsevier Publications Co.

Sahin, Sahin, H., & Peeters, F. M. (2013). Adsorption of alkali, alkaline earth and 3d transition metal atoms on silicene. *Physical Review B, 87*(8), 43–45.

Tkatchenko, A., Di Stasio, R. A., Car, R., & Scheffler, M. (2012). Accurate and efficient method for many-body van der wWaals interactions. *Physical Review Letters, 108*(23), 1–5.

Vogt, P., De Padova, P., Quaresima, C., Avila, J., Frantzeskakis, E., Asensio, M. C., et al. (2012). Silicene: Compelling experimental evidence for graphenelike two-dimensional silicon. *Physical Review Letter, 108*(15)*,* 1–5.

Yan, C., Ho Cho, J., & Ahn, J.-H. (2012). Graphene-based flexible and stretchable thin film transistors. *Nanoscale, 4*, 4870–4882.

Zacharia, R., Ulbricht, H., & Herte, T. (2004). Interlayer cohesive energy of graphite from thermal desorption of polyaromatic hydrocarbons. *Physical Review B, 69*(15)*,* 1–7.